The EMBO Journal Vol.2 No.11 pp.1901 – 1907, 1983

An extended secondary structure model for the TMV assembly origin, and its correlation with protection studies and an assembly defective mutant

David Zimmern

MRC Laboratory of Molecular Biology, Hills Road, Cambridge CB2 2QH, UK

Communicated by A.Klug
Received on 8 June 1983; revised on 16 August 1983

Recognition of the unique internal assembly origin on tobacco mosaic virus (TMV) RNA by the disk aggregate of the viral coat protein probably involves an extended region of the RNA (larger than that coated by a single disk) folded into a specific conformation. A secondary structure model is proposed for the RNA preferentially coated by limiting amounts of coat protein disks on the basis of partial nuclease digestion data. Part of this sequence can form three symmetrically spaced hairpins with marginally stable base paired sequences at the tips of the stems. The pattern of progressive protection of the RNA from nuclease attack during assembly suggests that these three hairpins are successively coated by the first three disks to add. The spacing of these hairpins is identical to that of three hairpins in the pseudo assembly origin (part of the coat protein gene homologous to the assembly origin). In Ni 2519, a TMV mutant whose assembly is defective at high temperature because it can no longer discriminate between the true and pseudo assembly origins, a point mutation has occurred near the tip of the third metastably base paired stem of the true assembly origin which would disrupt its structure and alter one copy of a repeated heptanucleotide. This suggests an important role for the ordered and cooperative recognition of successive loops in determining the specificity of assembly.

Key words: assembly origin/protein-nucleic acid interactions/RNA secondary structure/temperature-sensitive RNA/tobacco mosaic virus

Introduction

The assembly of tobacco mosaic virus (TMV) *in vitro* initiates at a unique internal site on the TMV RNA molecule ~1 kb from the 3′ end (reviewed by Klug, 1979). A two layered disk aggregate of 34 coat protein subunits binds to this site on the RNA, which is known as the assembly origin (O_a). The RNA at the assembly origin can form a stem and loop structure which is thought to intercalate between the layers of the initiating disk, thus facilitating cooperative nucleation stereochemically and contributing to the specificity of the reaction.

Although the outlines of this process are now fairly clear, some observations raise further questions. First, even when equal molar amounts of RNA and disks are mixed, nuclease digestion experiments show that only a proportion of the RNA molecules initiate assembly, and these are coated over a minimum of 300 bases corresponding to the addition of at least three disks (Zimmern and Butler, 1977; Zimmern, 1977). One interpretation of this is that several disks cooperatively recognise most or all of the preferentially encapsidated RNA sequence. Other evidence suggests that encapsidation of up to 20% of the genome may require disks (Shire *et al.*, 1981), and that specificity of initiation is lost when TMV RNA is fragmented beyond a certain point (Tyulkina *et al.*, 1975).

Secondly, when mixtures of RNase T1 partial digestion products of TMV RNA were incubated with disks, three adjacent fragments of the coat gene were selectively bound rather than the expected assembly origin fragments (Guilley *et al.*, 1975). The coat gene sequence at this point was shown to be partially homologous to that of the assembly origin (Zimmern, 1977), and this second site is now known as the pseudo assembly origin (ψO_a – Meshi *et al.*, 1981). Its resemblance to the true assembly origin is probably more than accidental. Certain TMV strains preferentially use an assembly origin within the coat protein gene (Fukuda *et al.*, 1980, and references therein). This resemblance is dramatically illustrated by a TMV mutant known as Ni 2519 which is temperature-sensitive in assembly (Jockusch, 1966; Bosch and Jockusch, 1972). Discrimination between O_a and ψO_a on Ni 2519 RNA breaks down *in vitro* at the restrictive temperature and assembly initiates at both sites simultaneously to form defective ribonuclease-sensitive particles comprising two nucleoprotein rods joined by a region of free RNA that cannot be coated (Taliansky *et al.*, 1982a; Kaplan *et al.*, 1982). A temperature-sensitive RNA could explain genetic observations suggesting that Ni 2519's defect in assembly *in vivo* is dominant and *cis*-acting (Taliansky *et al.*, 1982b). Because ψO_a is potentially functional and can be activated in Ni 2519 by raising the temperature or in the wild-type by fragmentation, the secondary or tertiary structure of the RNA molecule must be important to selective initiation on intact RNA.

Here, additional information from partial digestion studies of isolated RNA fragments from the assembly origin are combined with more extensive RNA sequence information to generate a secondary structure model of O_a extending previous models (Zimmern, 1977; Jonard *et al.*, 1977) in a 5′ direction (the major direction of assembly). The predicted structure includes three large symmetrically spaced stems and loops, whose successive protection from nuclease attack during partial assembly is consistent with their successive interaction with three coat protein disks. Secondary structure homology with ψO_a, together with sequence information showing that Ni 2519 carries a point mutation in the third (most 5′) of these loops (Zimmern and Hunter, 1983), suggest that cooperative recognition of the extended structure by successive coat protein disks contributes substantially to the specific nucleation of assembly.

Results and Discussion

The TMV assembly origin was operationally defined as the region of TMV RNA protected from nuclease digestion by limiting quantities of coat protein disks (Zimmern and Butler, 1977). A large number of partial digestion products of the free RNA from this preferentially protected region of 300 – 400 bases were isolated previously in the course of RNA sequence analysis. Those relevant to sequence determination of the smallest protected fragments were documented

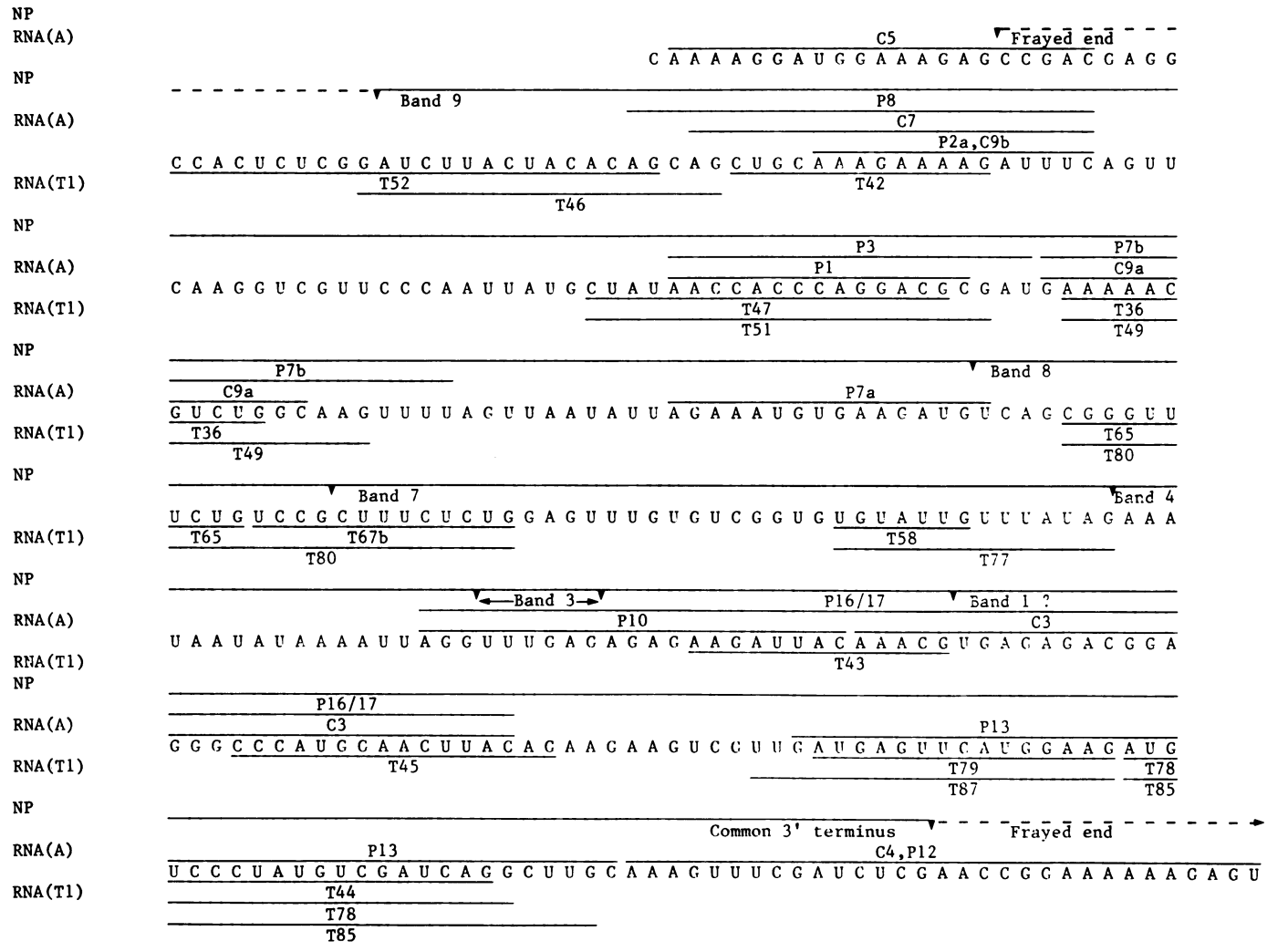

Fig. 1. Pattern of protection of the TMV assembly origin from nuclease attack by partial reassembly, and partial digestion products of the reextracted RNA. The nucleotide sequence shown extends from residue 5184 to residue 5556 of TMV RNA (Goelet *et al.*, 1982). Solid lines above the sequence labelled P- and C- denote pancreatic RNase A partial products [abbreviated RNA (A)], while solid lines below the sequence labelled T- denote RNase T1 partial products [abbreviated RNA (T_1)]. The pattern of nuclease cleavage of partly reassembled particles is shown on the top line (NP). The 5′ ends of each band isolated from nucleoprotein are numbered and indicated by an inverted triangle. To a first approximation all these bands have a common 3′ terminus at the point indicated. Lines are 49 residues long, the same as the number of nucleotides per helical turn in the particle, so that each successive line represents a successive turn.

previously (Zimmern, 1977), but many additional partial products derived from the remaining 5′ portion of the protected RNA where it proved impossible to overlap the entire sequence because of gaps where no partial products were obtained. The relevant RNA sequence has now been determined for several different variants of the wild-type, and, in part, for Ni 2519 (Goelet *et al.*, 1982; Meshi *et al.*, 1982; Zimmern and Hunter, 1983), so the complete set of partial digestion products (shown in Figure 1) can be used to identify nuclease-resistant parts of the sequence which are probably base paired.

As distinct from the products of partial digestion of free RNA reisolated from the partly assembled complexes, the end points of protection of RNA from attack by excess nuclease in the partly assembled nucleoprotein complexes define the pattern of coating of the RNA in the early stages of assembly. This information can be extracted by comparing the fingerprints of RNA fragments of various sizes resulting from assembly to different extents (Zimmern, 1977, Figure 4) with the completed sequence. The results of this analysis are also shown in Figure 1. Note that the resolution of this method differs for different fragments, since it depends on the disposition within the sequence of G residues (sites for cleavage by RNase T1, the nuclease used to remove uncoated RNA), and of unique RNase T1 or A oligonucleotides used to relate the sequence to the band fingerprints. In some fragments, the appearance of spots on the fingerprints in submolar yield suggests that the bands are mixtures of fragments with closely similar chain lengths but slightly staggered ends resulting from fraying at the end points of protection (for example band 3). For both these reasons the end points of the nucleoprotein can only be approximately located; the largest uncertainty (in band 4, due to a long G-lacking run) is 17 bases.

Secondary structure model

A secondary structure model (Figure 2) was constructed using the additional partial digestion information. The 200 bases at the 3′ end of this model most relevant to the immediate discussion are shown in Figure 2a. This structure comprises three large hairpins (stem and loop structures): the

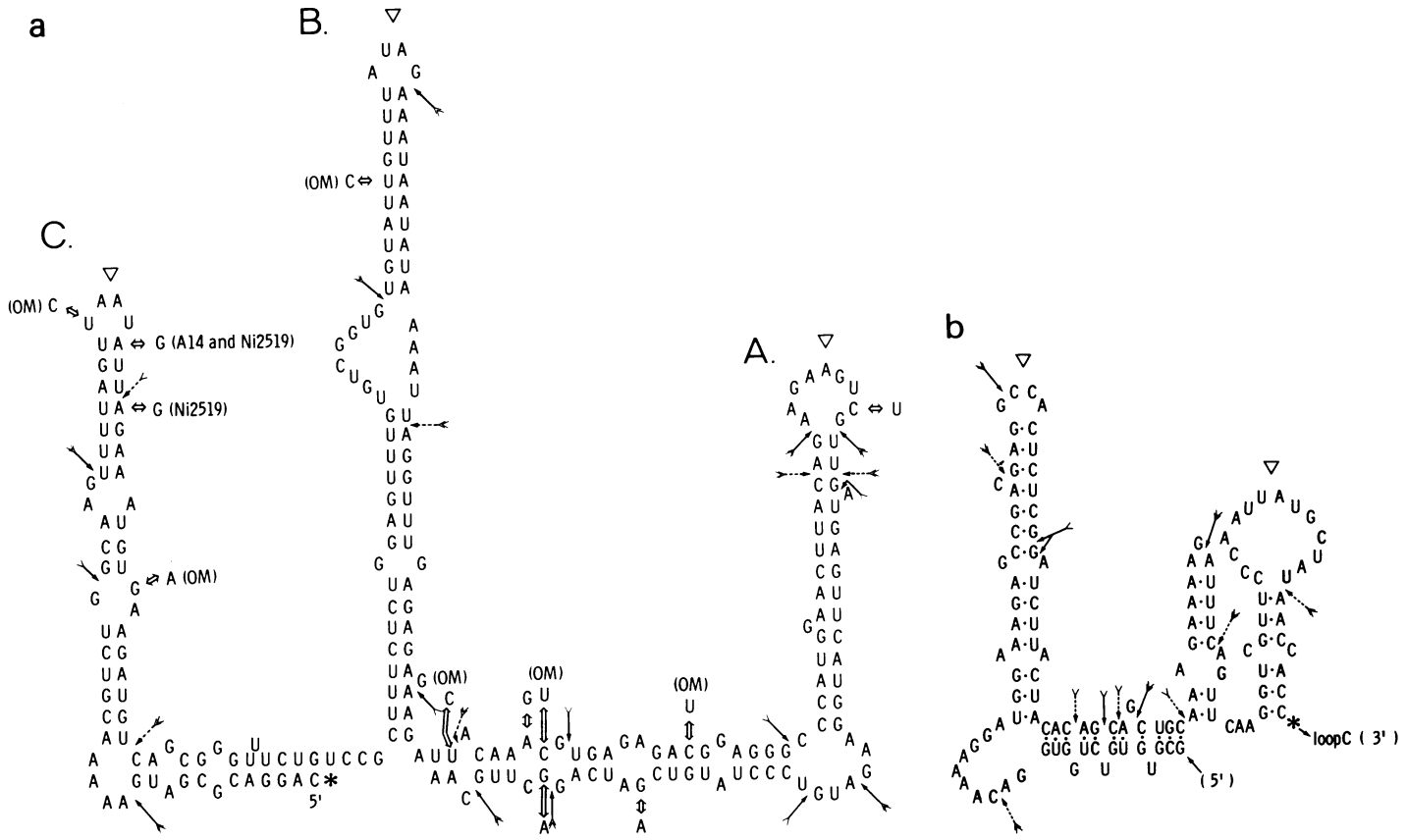

Fig. 2. (a) Secondary structure model of the 3′-terminal domain of the RNA sequence shown in Figure 1. Solid arrows indicate T1 RNase cleavage sites, dotted arrows pancreatic RNase cleavage sites. No partials were obtained spanning the sites indicated by the open inverted triangles, suggesting that these sites at the tips of the loops are very readily digested. Open double headed arrows denote base substitutions seen in various wild-type TMV stocks (where not otherwise identified), the closely related Japanese strain OM, the assembly defective mutant Ni 2519 and its parental strain A14. Hairpins A, B and C are defined in the text, each has a stem interrupted about halfway by a large asymmetric bulge: for purposes of the figure, stems A and C are shown bent at this point, but the true degree of distortion of stacking is unknown. [An alternative folding at the asymmetric bulge in stem B shown in Zimmern (1977) is also consistent with the partial digestion data, but leaves much of the 5′ side of stem B unpaired.] The * indicates the 5′ end where this domain joins that in **b. (b)** Secondary structure of the 5′-terminal domain of the RNA sequence shown in Figure 1. Symbols are as defined in **(a)**. The * indicates the 3′ end where this domain joins that in **a**.

one at the extreme 3′ end represents the core sequence found in the smallest partly assembled complexes which was therefore proposed to intercalate between the layers of the initiating coat protein disk (Zimmern, 1977). Quantitative protection extends well beyond this domain in a 5′ direction to include all the sequence shown in Figure 1, and for completeness, the structure deduced for the 5′-terminal portion of the protected region is shown in Figure 2b; this structure connects directly at its 3′ end to the structure shown in Figure 2a.

The partial digestion data from the isolated fragment population are well accounted for by the proposed structure, although it is always possible that more stable base pairing could be demonstrated in the intact RNA. There is some independent evidence for the existence of the structure in Figure 2a in intact RNA, however, since almost all the functionally neutral base substitutions seen in various wild-type TMV stocks (Zimmern, 1977; Jonard *et al.*, 1977; Meshi *et al.*, 1982) conserve the proposed base pairing; most sites of mutation either lying in loops or bulges or resulting in compensating double changes (Figure 2a). The main possible exception is a U to C transition towards the tip of the middle stem in strain OM (Meshi *et al.*, 1982), which would result in an A.C base pair. Such pairs, though destabilising, have been observed in tRNA stems.

The three large hairpins shown in Figure 2a, each with a large asymmetric bulge about half way down the stem, seem to form a domain with a high degree of symmetry. The three hairpin loops are spaced almost exactly the same distance apart (Figure 3, upper panel). Denoting the assembly origin (3′) hairpin as hairpin A, and the second and third successively 5′ to it as B and C, there are 78 nucleotides between loop A and loop B, and 75 nucleotides between B and C (Figure 3, upper panel). However, stem A is more stably base paired than the other two, which both terminate in short (10 and 7 bp, respectively) self complementary sequences lacking C residues (and consequently G.C pairs). Both these C-lacking tracts contain the sequence UAGAAAU, as was noted previously (Zimmern, 1977).

Partial secondary structure homology between O_a and ψO_a

A secondary structure model, also based on partial nuclease digestion, was previously derived for the pseudo assembly origin (Guilley *et al.*, 1975). Comparison of both proposed secondary structures revealed a striking feature – although there are four potential stems and loops in ψO_a three of these four loops have an identical spacing to that of the three loops in O_a (Figure 3).

Superimposed on the secondary structure homology bet-

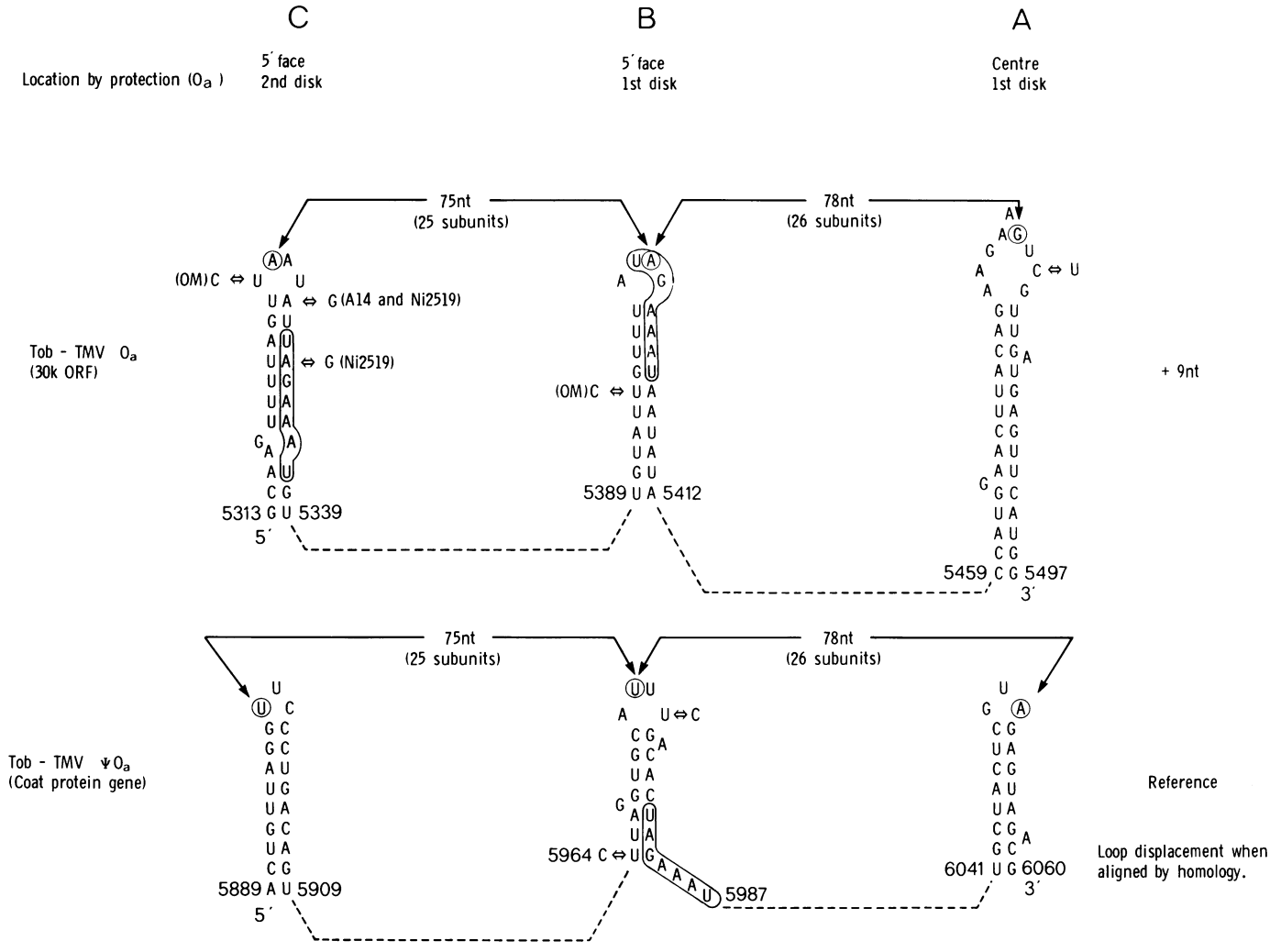

Fig. 3. Loop symmetry in the assembly origin. The upper panel shows the tips of hairpins A, B and C from the assembly origin of the common (tobacco) strain of TMV (cf. Figure 2a). The corresponding hairpin tips from the pseudoassembly origin are shown in the bottom panel. These domains lie within the 30-K open reading frame (ORF) and the coat protein gene, respectively – nucleotide residue numbers from the sequence of Goelet *et al.* (1982) are shown. Residues connecting the hairpin tips, symbolised by the dotted lines, have been omitted. ΨO_a shows nucleotide sequence homology to O_a, but when the sequences are aligned, each hairpin is displaced by 9 residues relative to the corresponding hairpins in the other sequence. The symmetrical arrangement of the hairpins is displayed by measuring the distance between bases in the first position of the genetic code nearest the tips of the loops; a convention adopted to compare loops of different sizes. Since each TMV coat protein subunit binds three bases this equals the number of subunits required to coat the RNA from loop to loop, although the choice of phase is arbitrary.

ween O_a and ΨO_a is a primary sequence homology. Both hairpins B contain the heptanucleotide UAGAAAU, although its position relative to the terminal loop is not identical in both cases. If the two sequences are aligned for maximum homology of primary sequence, equivalent secondary structures (the loops) in Oa are displaced ~9 nucleotides 5′-wards compared with those in ΨOa. Assessment of the significance of this repetition with respect to assembly is complicated by the fact that it may be important to protein function, since both O_a and ΨO_a lie within open reading frames on TMV RNA. All three copies of UAGAAAU in O_a and ΨO_a are identically aligned with their respective translational reading frames, the last six bases specifying Arg-Asn. The Arg-Asn sequence in the coat protein is conserved in all strains and mutants of TMV, and is thought to be involved in binding one of the three RNA phosphates per subunit (Klug, 1979). There is one other copy of the sequence UAGAAAU at positions 5613–5619 on TMV RNA (Goelet *et al.*, 1982), which also encodes Arg-Asn, but there is no evidence at present to connect this with assembly initiation at either O_a or ΨO_a.

Does this symmetrical array of hairpin loops have anything other than a geometrical significance? Guilley *et al.* (1975) first isolated fragments corresponding to hairpins A, B and C from ΨO_a as separate products of partial T1 RNase digestion recovered from binding reactions with coat protein disks. Although it was not entirely clear from their data that all three fragments could bind independently, since rebinding of isolated fragments was not checked, and A, B and C are originally contiguous fragments isolated following a nuclease step, their observations are consistent with a model in which loops B and C are reinforcing disk binding site. This is supported by the protection data.

Correlation of the proposed secondary structure with protection experiments

Within the limits of resolution already noted, it appears on comparing the end points of RNA fragments protected from nuclease digestion to different extents by coating with pro-

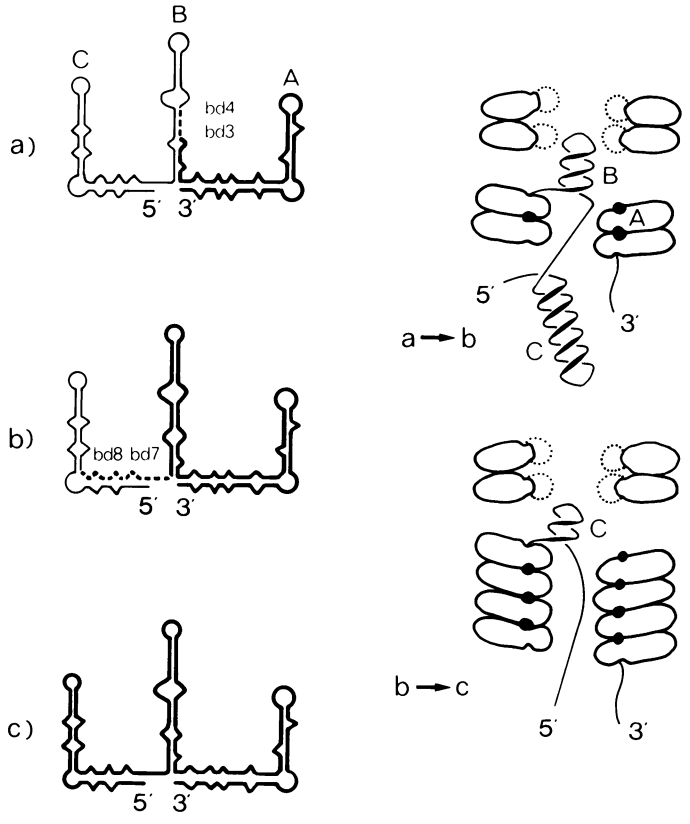

Fig. 4. Correlation of protection against nuclease attack with secondary structure, and a model for cooperative nucleation of assembly. The 5′ end points of bands 3 and 4 (corresponding to protection by one disk) and bands 7 and 8 (corresponding to protection by two disks) are shown in **(a)** and **(b)**, respectively, superimposed on schematic outlines of the secondary structure (protected region is the heavy line). Bands 4 and 8 are 5′-terminal extensions of bands 3 and 7 (additional sequences shown dotted), which probably represent frayed derivatives of the former due to resection of RNA lying on the 5′ face of the disk. In **(c)** the entire domain is protected, corresponding to band 9 which spans it completely. An interpretation of the disposition of hairpins A (coated), B (migrated through the central hole and the base of the stem unwound leaving only the tip base paired) and C (fully base paired) after binding the first disk is shown on the right in the form of an axial section **(a→b)**. **(b→c)** illustrates their postulated arrangement after binding the second disk. These diagrams are intended only to help visualise the process since many details are still unclear, for example we do not know when the disk dislocates.

gressively more protein (Figure 1) with the secondary structure model (Figure 2) that each of the first three disks to add protects successive hairpins. In the most abundant of the minor protected fragments corresponding to the addition of the first disk (band 4, Figure 1), protection extends from at least residue 5419 halfway up the 3′ side of stem B to residue 5540 beyond the base of stem A on the 3′ side (Figure 4a). The size of band 4 (121 bases) compared with the maximum number that could contact a single disk (3 bases/subunit x 17 subunits/turn x 3 turns = 153 bases) suggests that RNA bound both between layers of a disk and on either face is protected to some extent against nuclease attack. The next smaller fragment (band 3) is a truncated version of band 4 corresponding closely to stem A (Figure 4a). Such information as is available on one smaller band locates its 5′ end point on the 3′ side of residue 5443, suggesting that fraying can extend some distance along the 5′ face of the disk, and that this is the side on which the RNA is least well protected.

The major fragments in the next larger size class are bands 7 and 8. In band 8, protection extends 5′-wards to residue 5350, including all of stem B and half of the 3′ side of stem C, ending opposite the asymmetric bulge (Figure 4b). Note that due to the favourable disposition of unique RNase T1 and A end products (UCAG and GAAGAU, respectively) this end point can be located to within a few bases. It implies that protection ends at a very similar position with respect to the secondary structure as with band 4 on stem B, though the latter locates the protected sequence less accurately. Band 7 resembles band 3 in being a truncated version of the major band (Figure 4b).

In the next larger fragment, band 9, protection has extended 5′-wards for more than 140 bases to approximately residue 5200, including all of loop C and substantial additional sequence. Although the 5′ end point of this fragment does fall within the major potential stem and loop structure to the left of loop C (Figure 2b), this loop is not symmetrically spaced with respect to the first three. It is not clear whether or not the large gap between bands 8 and 9 is an artefact due to the fact that small (band 8 and smaller) and large (band 8 and larger) fragments were prepared in slightly different ways, with consequent underrepresentation of intermediate sized bands. All the digestion products characteristic of band 9 occur in digests of the unfractionated population of fragments protected at equimolar disk:RNA ratios in close to molar yields, suggesting that assembly up to this point is highly cooperative.

A point mutation in loop C of the assembly origin in mutant Ni 2519

TMV temperature-sensitive mutant Ni 2519 is defective in assembly at 33°C, and forms defective particles *in vitro* at this temperature due to initiating assembly simultaneously at O_a and ψO_a (Bosch and Jockusch, 1972; Taliansky *et al.*, 1982a, 1982b; Kaplan *et al.*, 1982). Two point mutations (both A to G transitions) are found close to the assembly origin in Ni 2519 RNA compared with the type sequence, at positions 5329 and 5332 in the RNA (Zimmern and Hunter, 1983). That at position 5329 is also found in the thermostable parental strain of Ni 2519, known as A14, but that in position 5332 is not. Since the latter mutation reverts to the parental sequence when progeny are selected that form mature virus at 33°C, it is very probably associated with the temperature-sensitive assembly of Ni 2519. Further mutations cannot be entirely ruled out in hairpin A of O_a or in ψO_a of Ni 2519, although these would have to be translationally redundant mutations since no alterations corresponding to these locations are detectable by peptide mapping of translation products.

Comparison of the sites of these substitutions with the secondary structure model shows that the A to G transition at residue 5332 in Ni 2519 alters the sequence of the repeated heptanucleotide UAGAAAU towards the tip of stem C of O_a to UGGAAAU (Figures 2a and 3). A primary sequence alteration alone might affect assembly in a *cis*-dominant fashion in one of two ways: by perturbing the cooperative binding of coat protein, or by altering the binding site for a catalytic factor required in assembly. However, the former effect would probably be small relative to the binding energy of bases already coated by that point (Steckert and Schuster, 1982), while there is no evidence so far for the involvement of other proteins, although a minor catalytic factor might have escaped detection. On the other hand, when secondary structure is also taken into account, the two A to G transitions at

positions 5329 and 5332 would weaken the base pairing of the self-complementary C-lacking tract at the tip of hairpin C to the point where its stability can only be marginal, if it survives at all (Figures 2 and 3), and this could explain a temperature-sensitive defect of the RNA.

The A to G change between wild-type TMV and A14 alters the A-U base pair at the top of stem C (U 5324:A 5329) to a G-U pair, but free energy calculations using the supplemented version of Tinoco's rules compiled by Salser (1977) show that this change alone should make relatively little difference to the melting temperature of the hairpin. The free energy of formation of the two terminal base pairs is so nearly equal to the energy penalty incurred in forming a terminal loop of four rather than eight bases as to be within the margin of error of the calculations. In contrast, the additional mutation in Ni 2519 replaces one of the two A-U base pairs stacked in opposite orientations in the middle of the terminal 7-bp segment of stem C (U 5321:A 5332) with a G-U pair. These two A-U base pairs make the largest single contribution (-1.8 kcal) to the stability of this segment of the stem; the mutation reduces this to -0.3 kcal. It also seems likely that the progressive substitution of all but three A-U pairs by G-U wobble base pairs in a stem of at most seven bases may create cumulative steric difficulties and disrupt this segment of the stem altogether. However, the overall free energy sum (at 25°C) calculated assuming a 14-bp stem from the large asymmetric bulge to an 8 base terminal loop is still negative (-5.1 kcal at 25°C). While the free energy calculations are approximate and the effect is small, the relative stabilities calculated would clearly be compatible with a model in which melting of the terminal segment of loop C affected initiation of assembly on Ni 2519 RNA at a lower temperature than either wild-type virus or A14 (the restrictive temperature for Ni 2519 is 33°C, while wild-type virus does not replicate well at temperatures above 37°C). Whether it is the only factor remains to be determined.

A model for cooperative assembly nucleation

The terminal portions of stems B and C are weakly base paired in O_a, containing only A-U and G-U base pairs since they are formed from C-lacking tracts. A slightly divergent Japanese wild-type strain known as OM which contains several substitutions in O_a has two C residues interrupting these C-lacking tracts, one in loop C and the second in stem B (Meshi *et al.*, 1982). However, neither C residue is paired with a G, suggesting possible selection against G.C base pairs rather than C residues themselves. The effects of the Ni 2519 mutation, on the other hand, suggest that further weakening of the base pairing at the tip of stem C may cause temperature-sensitive assembly. These observations can be reconciled by assuming that the assembly mechanism requires that the melting temperatures of the distal portions of stems B and C be constrained within a relatively narrow range. Taken together with the regular loop spacing and correlation with the pattern of protection, these observations suggest a model in which the two small, C-lacking stems at the tips of hairpins B and C successively melt, pass through the central hole of the nucleation complex, and reform on the other side, where they would be strategically placed to interact with the second and third disks to add, respectively. This could either involve intercalation between the layers of the second and third disks in a manner similar to that involved in nucleation by the first disk, or simply a lining up of successive disks using the hairpin loops as a guide to align the incoming disks (Figure 4, right panel). In this picture, the reformation of a stem-loop hairpin structure after passing through the central hole of the next disk may only involve the tips of the hairpins, so that part of the sequence may lie on the top surface of the previous disk. This would account for the fraying in the nuclease protection pattern.

This model is consistent with the following observations. First, nucleation complexes formed at limiting protein ratios preferentially result from the addition of at least three disks. Second, end points of fragments protected from nuclease digestion by addition of limiting amounts of coat protein are consistent with successive protection of loops A, B and C (Figure 4). It is interesting to note that while the loops are spaced 75–80 residues apart, the digestion end points still tend to align in register with the periodicity of the viral helix, as can be seen from Figure 1 where each line is 49 nucleotides long and thus corresponds to one turn of the helix. Consequently the spacing between bands 3 and 7, representing protection of loop B, is ~50 bases rather than 102 as expected for protection by all 34 subunits of a disk. This suggests that not all of the subunits of the second disk are incorporated into the nucleation complexes. It is not yet clear if this is a feature peculiar to nucleation, perhaps reflecting coupling of cooperative nucleation by several disks to the disk to helix quaternary structure transition, or if it is also true of larger growing rods. Butler and Lomonossoff (1978) observed intervals between much larger bands protected from nuclease digestion at higher protein input ratios, some of which were ~50 rather than 100 bases. Third, the model can at least begin to explain the breakdown in accurate selection of the true assembly origin over the pseudo assembly origin in Ni 2519 at the restrictive temperature since loop C in ψO_a of Ni 2519 is significantly destabilised: it may be necessary to strike a balance between easy melting of the nucleation region on one side of the disk and reforming the loops on the other, hence discrimination could be temperature-dependent. However, the model cannot yet explain why ψO_a is activated in Ni 2519 at high temperature, but not in the wild-type virus: sequencing of ψO_a may shed light on this point. In summary, I suggest that the conformation of the assembly nucleation region, specifically the disposition of at least three regularly spaced hairpin loops, is important to the specificity of recognition by the viral coat protein in a cooperative reaction.

Materials and methods

Isolation of assembly nucleation complexes, extraction of protected RNA, and partial digestion procedures were documented previously (Zimmern and Butler, 1977; Zimmern, 1977).

Acknowledgement

I would like to thank Aaron Klug for his constructive criticism and encouragement.

References

Bosch,F.X. and Jockusch,H. (1972), *Mol. Gen. Genet.*, **116**, 95-98.
Butler,P.J.G. and Lomonossoff,G.P. (1978) *J. Mol. Biol.*, **126**, 877-882.
Fukuda,M., Okada,Y., Otsuki,Y. and Takebe,I. (1980) *Virology*, **101**, 493-502.
Goelet,P., Lomonossoff,G.P., Butler,P.J.G., Akam,M.E., Gait,M.J. and Karn,J. (1982) *Proc. Natl. Acad. Sci. USA*, **79**, 5818-5822.
Guilley,H., Jonard,G., Richards,K.E. and Hirth,L. (1975) *Eur. J. Biochem.*, **54**, 135-153.
Jockusch,H. (1966) *Z. Vererbungsl.*, **98**, 320-343.
Jonard,G., Richards,K.E., Guilley,H. and Hirth,L. (1977) *Cell*, **11**, 483-493.

Kaplan,I.B., Kozlov,Yu.V., Pshennikova,E.S., Taliansky,M.E. and Atabekov,J.G. (1982) *Virology,* **118**, 317-323.
Klug,A. (1979) *Harvey Lectures,* **74**, 141-172.
Meshi,T., Ohno,T. and Okada,Y. (1982) *J. Biochem.,* **91**, 1441-1444.
Salser,W. (1977) *Cold Spring Harbor Symp. Quant. Biol.,* **42**, 985-1002.
Shire,S.J., Steckert,J.J. and Schuster,T.M. (1981) *Proc. Natl. Acad. Sci. USA,* **78**, 256-260.
Steckert,J.J. and Schuster,T.M. (1982) *Nature,* **299**, 32-36.
Taliansky,M.E., Kaplan,I.B., Jarvekulg,L.V., Atabekova,T.I., Agranovsky, A.A. and Atabekov,J.G. (1982a) *Virology,* **118**, 309-316.
Taliansky,M.E., Atabekova,T.I., Kaplan,I.B., Morozov,S.Yu., Malyshenko,S.I. and Atabekov,J.G. (1982b) *Virology,* **118**, 301-308.
Tyulkina,L.G., Nazarova,G.N., Kaftanova,A.S., Lednova,R.K., Bogdanov, A.A. and Atabekov,J.G. (1975) *Virology,* **63**, 15-29.
Zimmern,D. (1977) *Cell,* **11**, 463-482.
Zimmern,D. and Butler,P.J.G. (1977) *Cell,* **11**, 455-462.
Zimmern,D. and Hunter,T. (1983) *EMBO J.,* **2**, in press.